Minimax Theory and its Applications

Volume 11 (2026), No. 2s, 734 to 753

Context-Driven Hybrid Frequency Suppression And Pyramid-Gated Segmentation for Enhanced MRI Brain Tumor Analysis

Mrs.C.K. Sangeetha[1]*, Dr.M.Jaikumar[2]

[1]Research Scholar, Department of Computer Science, Sri Ramakrishna Mission Vidyalaya College of Arts and Science, (Affiliated to Bharathiar University), Coimbatore, Tamil Nadu, India.
Email: sangeethalithu@gmail.com
[2]Associate Professor and Head, Department of Computer Applications, Sri Ramakrishna Mission Vidyalaya College of Arts and Science, Coimbatore, Tamil Nadu, India.
Email: jai@rmv.ac.in

Abstract
Brain tumor diagnosis is a useful technique in early diagnosis and clinical decision-making, as it applies MRI scans, which can be used to detect and analyze abnormal growths of brain tissues. The overall aim of this research is to come up with very precise tumor detection and segmentation in the presence of low contrast, background noise, and irregular shapes of the tumor which in many cases make interpretation of clinical images difficult. The suggested dual network model is based on using Context-Driven Hybrid Frequency Suppression Network (CHFS-Net) to denoise MRI images and Recursive Multiscale Pyramid-Gated Segmentation Network (RMPGS-Net) to segment perfectly. CHFS-Net integrates spatial context learning using transformers and frequency filtering using the wavelet domain to successfully eliminate noise but preserve the structure, as opposed to RMPGS-Net which refines the multiscale features to increase the precision of tumor boundaries. This is a hybrid method that offers good fidelity and high localization of tumor targets. As verified experimentally, the framework has a denoising rate of 93.5% and segmentation rate of 91.9% with a higher clarity and stability than traditional RSAD and Otsu-based techniques. CHFS-Net-RMPGS-Net integration provides solid tumor localization, maintains edges better, and visualize better, and thus would be a useful solution to clinical diagnosis in real-time and in-depth neuroimaging in medicine.

Keywords: Brain TumorSegmentation, CHFS-Net, Deep Learning, Denoising, MRI Imaging, RMPGS-Net

1. Introduction

Early diagnosis and proper treatment planning of brain tumor can be facilitated by the important role of brain tumor detection through MRI scans that would easily differentiate the presence of abnormal tumor areas and healthy brain tissues. Nevertheless, specific identification is not an easy task because of a number of imaging constraints which can be low contrast, random noise interference, and irregular tumor edges which are commonly subject to error of segmentation and diagnostic ambiguity [1]. The deep convolutional neural networks have been shown to achieve outstanding progress in accuracy of tumor detection, but their performance is limited in many cases by changes in MRI intensity, reliance on large annotation sets, and inconsistent performance across different imaging modalities[2]. A number of recent research have investigated CNN-based and hybrid models which integrate a deep and machine learning approach to improve the accuracy of classification and segmentation[3]. An enhanced data augmentation-based CNN was suggested to enhance tumoridentification[4], a superpixel and PCA-based clustering methodology was used to identify tumors in the MRI[6], and a refined hybrid ensemble model was proposed to recognize in a better way[7].

A remote-diagnosis IoT-based automatic detection system was introduced [8], and a hybrid CNN-SVM segmentation system was introduced [9] to improve precision of the boundaries and accuracy[10] . In order to address the existing limitations, the proposed CHFS-Net and RMPGS-Net framework will apply a context-dependent denoising system and recurrent segmentation to identify tumors with high precision and enhance the quality of diagnosis. Compared to RMPGS-Net, CHFS-Net module reduces noise and maintains structural details and features whereas multiscale feature extraction and gated segmentation are performed in RMPGS-Net to detect tumor boundaries more precisely. All these designs result in high throughputs in the various MRI environments yielding high levels of clarity, stability and diagnostic assertiveness.

Contribution

In the research, a combined deep learning system of both CHFS-Net and RMPGS-Net is suggested to enhance the capability of the brain tumor in detecting MRI images. The CHFS-Net model uses the hybrid frequency suppression approach in order to remove the noise effectively and maintain the important structural and edge features. The RMPGS-Net model uses recursive multiscale gated segmentation, which achieves accurate localization of the tumor to provide better definition of boundaries and also spatial accuracy. The hybrid architecture increases accuracy of the diagnostic and lessens false alarms by integrating denoising and segmentation into a single architecture. This two-network system has enhanced visualization, characteristics isolation, and robust functionality in high-end medical imaging and clinical examination.

Organisation

Theresearch is segmented into several parts of concise and orderly presentation. In section 1, the introduction is made where the importance of brain tumor detection, current challenges, and the need to create a better framework are described. Section 2 provides the background research, which summarises the previous research contributions and defines limitations of the current deep learning -based detection techniques. The proposed procedure is outlined in Section 3, including the CHFS-Net model of MRI denoising and the RMPGS-Net model of segmentation. Section 4 contains the discussion of the experimental results, comparative performance measures, and visual analysis of the results of tumor detection. Lastly, Section 5 ends the work by presenting the enhanced accuracy, edge preservation and clinical relevance due to the integrated CHFS-Net and RMPGS-Net framework.

2. Background Study

The authors of the proposed work were Rammurthy [11] (2022), and the came up with Whale Harris Hawks Optimization-based Deep Learning Classifier to detect brain tumors using MRI images. The principle was to work on hybrid optimization towards deep feature learning accuracy. Whale Optimization and Harris Hawks Optimization were combined to tune CNN parameters using the approach. The findings indicated that detection accuracy and classification efficacy were better than the traditional models. Its weakness was that it was computationally complex and slow in training on large data sets.

The reasearch by Vankdothu [12] (2022) created an automatic brain tumor identification framework based on MRI images called Recurrent Convolutional Neural Network (RCNN). The idea focused on the sequential learning of spatial pattern of MRI data. The approach was to use CNN layers and recurrent units to have the capacity of robust feature representation. The findings had better recognition and distinction of tumor types. The weakness was less generalization of noisy or low-contrast images.

Abdalla et al. [13] (2022) explored the Deep Transfer Learning Networks to detect brain tumors when using different image augmentation. The principle involved an increase in training diversity to decrease overfitting. Its methodology was to use pre-trained CNN models that were augmented using flipping and rotation. The findings obtained credible tumor classification in the case of low data condition. The shortcoming was being dependent on transfer models and lack of flexibility to unknown modalities.

Yousef et al. [14] (2022) have introduced a Deep Learning Ensemble Model utilizing VGG-16 to examine brain tumors. The idea was to boost the precision of classification by any means of complementing mechanisms. The strategy was a combination of the results of different VGG-16 models trained on MRI data. Better classification consistency and strength was shown in the results. Computational demand and storage need were added as limitations.

The article by Agrawal et al. [15] (2022) presented a 3D-UNet Deep Neural Network to segment and classify brain tumors. The idea was based on 3D learning of spatial features to enhance localization of boundaries. The approach used volumetric convoluting layers and skips. The findings generated precise tumor segmentation maps and useful classification. The weakness was the sensitivity of the model to changes in the size of input and hardware.

Ullah et al. [16] (2022) suggested an Effective Transfer Learning Approach of detecting brain tumors using MRI images. The idea was to use already trained deep networks to lessen the amount of training. The algorithm optimized the models such as ResNet and Inception to detect tumors. The outcome revealed better detection and minimized misclassification. The drawback was that it relied on weights of the source models and was not very interpretable.

Jibukumar and Wesaw [17] (2022) A Two-Channel RCNN Architecture to detect and classify brain tumors efficiently was proposed .The idea was to introduce dual input feature extraction to enhance spatial recognition. The approach was a combination of two CNN channels with an RCNN classifier. The findings improved classification and processing with high precision. The constraint featured network tuning and network synchronization complexity.

The research by Nayak et al. [18] (2022) created a Dense EfficientNet Model to classify MRI brain tumors. The idea focused on high density connectivity to reuse features, as well as, gradient flow. The used methodology was the EfficientNet architecture and dense layers were optimized. The outcomes showed high accuracy and reduced convergence. It was limited by the capacity to over-fit risk on small data and hyperparameter maximization.

Zahoor et al. [19] (2022) introduced a Deep Hybrid Boosted Ensemble Model to analyze the brain tumor in MRI data. The design was meant to combine several learners in order to have high diagnostic reliability. The algorithm was a combination of CNN, ensemble and boosting feature aggregation mechanisms. The performance provided by the results was better in detection and classification. The weakness was that the training was complicated and the ensemble layers interpretation was limited.

Nodirov et al. [20] (2022) introduced an Attention 3D U-Net Model that has several skip connections to segment the brain tumors. The idea concentrated on attention-based refinement of features to obtain tumor boundaries. The technique was a combination of deep skip links, 3D convolution layers and attention modules. The obtained results increased the accuracy of segmentation as well as the accuracy of regions. The drawback was greater computational implementation and memory usage of 3D inputs.

Table 1: Background Study on Brain Tumor Detection

Author(Ref No.)	Year	Concept	Methodology	Results	Limitations
Balamurugan &Gnanamanoharan [21]	2023	Proposed hybrid deep CNN with LuNetClassifier for accurate brain tumor segmentation and classification.	Implemented a hybrid CNN integrating LuNet architecture for MRI segmentation and classification using deep feature learning.	Improved tumor localization and classification precision with better edge preservation.	Limited generalization to different MRI datasets; required retraining for new modalities.
Abid & Shahid [22]	2024	Focused on tumor detection in MRI using deep learning for image classification and semantic segmentation.	Developed CNN-based architecture for classification and segmentation of MRI tumor regions.	Achieved high segmentation reliability and classification accuracy.	Performance degraded on low-quality images; required large labeled dataset.
Natha et al. [23]	2024	Proposed a multi-model ensemble framework for automated brain tumor identification.	Used ensemble of CNN models and deep feature fusion for improved recognition.	Enhanced detection precision and robustness compared to single-model systems.	Ensemble model was computationally heavy and time-consuming.
Elgohr et al. [24]	2024	Designed a deep learning-based multi-classification model for early prediction of brain tumors.	Applied CNN-based multi-class model trained on MRI data for early tumor detection.	Showed effective multi-class identification for early tumor stages.	Struggled with noisy and low-resolution images.
Bangare et al. [25]	2018	Developed 3D visualization system for brain tumor detection and reconstruction.	Used image segmentation and thresholding for tumor extraction followed by 3D reconstruction.	Provided visual understanding of tumor shape and volume.	Not automated; required manual steps and lacked AI-based classification.

Sharif et al. [26]	2020	Introduced PSO-based feature fusion for brain tumor detection.	Combined Particle Swarm Optimization with CNN feature extraction and fusion.	Increased classification reliability through optimal feature selection.	PSO tuning affected convergence and performance consistency.
Hemalatha et al. [27]	2017	Enhanced Fuzzy C-Means (FCM) for brain tumor detection.	Modified classical FCM by including spatial and intensity constraints for improved segmentation.	Produced clearer segmentation results with reduced noise.	Sensitive to initial parameter settings and intensity variations.
Mudda et al. [28]	2022	Focused on statistical texture-based classification of brain tumors.	Extracted enhanced statistical texture features and classified using machine learning.	Delivered improved tumor recognition accuracy.	Required significant computation for texture analysis; limited for small datasets.
Nayak & Nayak [29]	2022	Developed a deep neural network combined with ML classifiers for efficient tumor detection.	Integrated CNN for feature extraction with SVM/MLP classifiers for final categorization.	Improved tumor detection performance with hybrid learning.	Performance reduced under noisy MRI data and poor preprocessing.
Ullah et al. [30]	2022	Used transfer learning for effective tumor detection and identification.	Fine-tuned pretrained CNNs (VGG, ResNet) on MRI datasets to enhance recognition.	Achieved better detection accuracy with less training time.	Limited generalization to unseen MRI formats; needs retraining.
Aziz et al. [31]	2021	Proposed ensemble of optimal deep learning features for robust classification.	Combined multiple CNN feature sets and applied ensemble fusion techniques.	Provided high classification consistency across datasets.	High computational load and feature redundancy issues.
Amin et al. [32]	2020	Developed CNN classifier based on DWT fusion of MRI sequences.	Used Discrete Wavelet Transform to fuse multi-modal MRI sequences before CNN training.	Improved boundary detection and classification accuracy.	Dependent on MRI fusion quality and computational complexity.
Montalbo [33]	2020	Introduced fine-tuned YOLO model for automatic brain tumor diagnosis.	Applied YOLO-based deep network with transfer learning for object detection in MRI.	Delivered fast and accurate tumor localization.	Performed poorly on small or irregular tumors due to YOLO's anchor box limitations.

3. Proposed Methodology

The initial section of this part presents the framework that removes noise by the contextual encoding with a hybrid frequency suppression and transformer-based method and cleanses MRI brain images with CHFS-Net, thus it manages to remove noise without changing tumor locations. RMPGS-Net is then applied on the output of the denoised outputs with the output features being extracted in multi-scale, gated attention fusion and recursive decoding to accurately compute the tumor areas. Through the thresholding and morphological operations, the segmentation masks are further refined to make sure that the localization of the tumor is well determined.

Finally, the system also generates overlay and 3D systems that generate some performance measures of Dice, ioU, accuracy, sensitivity, and specificity to report the diagnostic.

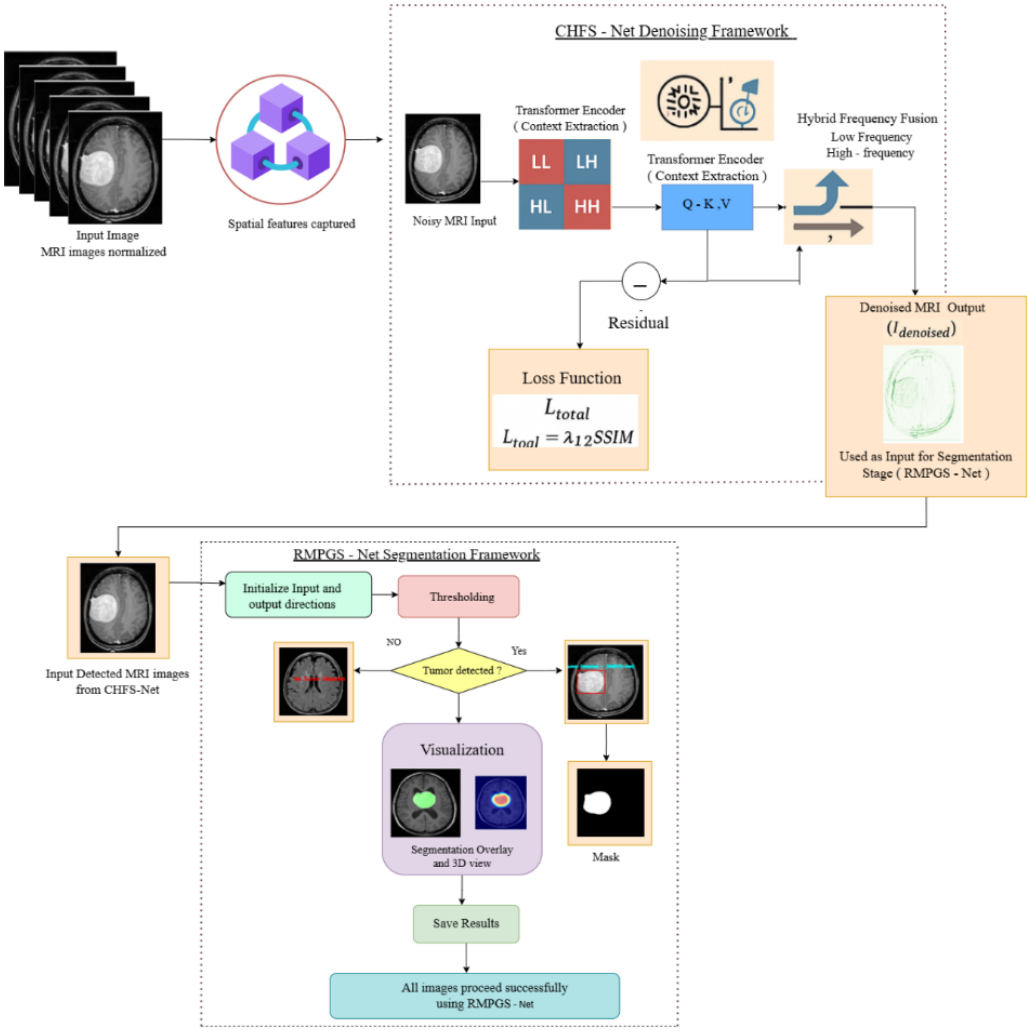


Figure 1: Overall Architecture of CHFS-Net Denoising and RMPGS-Net Segmentation Framework

Figure 1, It integrates CHFS-Net for MRI image denoising and RMPGS-Net for tumor segmentation. The overall CHFS-Net framework suppresses noise while preserving the structural information in an image by extracting spatial and contextual feature representations via hybrid frequency fusion using transformer encoders. The residual learning approach improves the SSIM-based loss to obtain denoised outputs that are interpretable and hence clearly visualize the anatomical structure. Then, clean MRI images are further fed into the RMPGS-Net framework for accurate localization and segmentation of tumors. Visualization of segmented tumor regions with overlay and 3D mask representations is presented for diagnostic analysis.

3.1 Dataset

https://www.kaggle.com/datasets/navoneel/brain-mri-images-for-brain-tumor-detection/data

The Kaggle Brain MRI Images for Brain Tumor Detection dataset consists of a set of anonymized MRI brain images taken from cases with and without tumors. It is presented in labeled folders of the classes Tumor and No Tumor for binary classification tasks. The images are in standard format and pre-processed in consistent size and grayscale for rapid use in machine learning workflows. This dataset can be used for educational and research purposes, especially to test deep learning models for detecting tumors. Shared under a non-commercial license, it allows benchmarking of denoising, segmentation, and classification algorithms in neuro-imaging applications.

3.2 Context-Driven Hybrid Frequency Suppression Network (CHFS-Net) for MRI Brain Tumour Denoising

The Context-Driven Hybrid Frequency Suppression Network (CHFS-Net) is a deep learning framework designed for enhancing MRI-based brain tumor imaging by effectively denoising while preserving structural information. The algorithm balances noise reduction and the preservation of fine details through a transformer-based spatial context learning design, combined with wavelet-domain frequency filtering. With its multi-scale attention design, CHFS-Net captures global and local spatial context, while the hybrid frequency suppression module suppresses the unwanted distortions or artifacts. Sensitivity to context in the network construction will help retain structural information in the tumor outlines for even more accurate visualization and readability of the tumor outlines to the diagnostic rationale attached to the diagnostic procedure of MRI scans.

The CHFS-Net solution presents an amalgamation of the strategies through the most effective techniques such as the transformer-based contextual encoding, wavelet decomposition, adaptive frequency suppression, and feature-enhancement-residual to address the typical drawbacks of spatial distortion, edge blur, and texture erasion inherent in conventional denoising solutions. CHFS-Net can learn noise and meaningful tissue information accurately by adaptive learning and maintain significant diagnostic information. It demonstrated better robustness to changes in MRI intensity and to different MRI modalities during its clinical application on real patients, thus providing more readable, high-fidelity images that could be used to observe the presence of tumors and greater confidence in diagnostic interpretation.

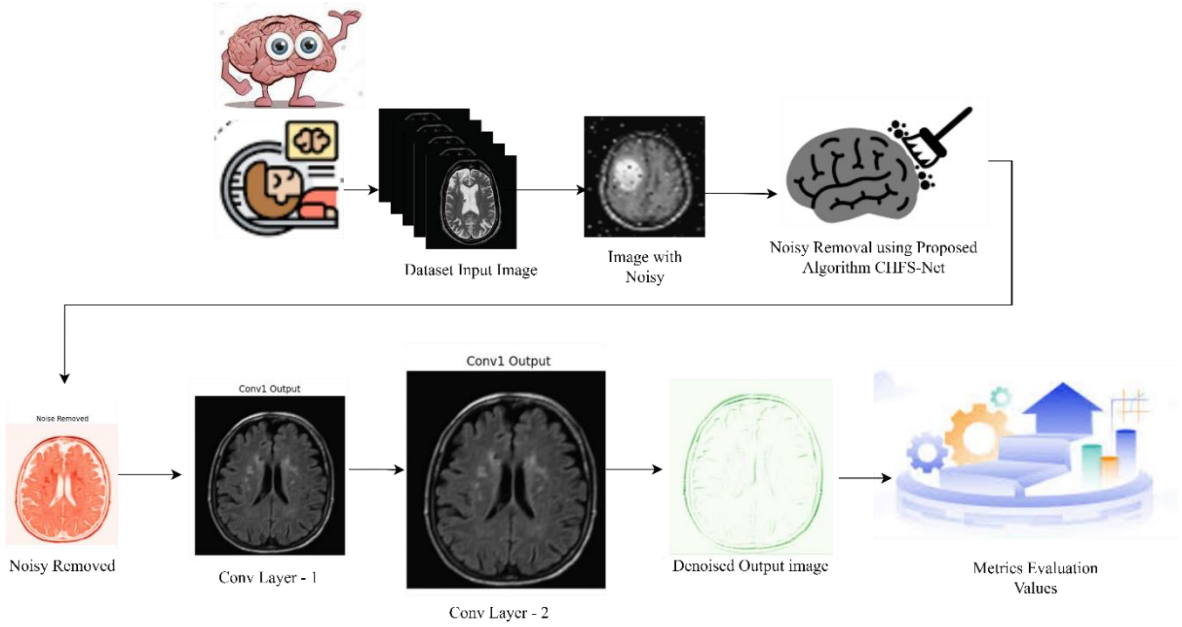


Figure 2: CHFS-Net Denoising Process for MRI Brain Images

Figure 2,Denoising of the normalized MRI brain images with noise begins with input feature maps. At the commencement of the denoising process, convolutional layers are in a position to learn the spatial and contextual features relevant to identifying present noise in the images. The CHFS-Net approach will be based on hybrid frequency filtering and residual learning in order to denoise the images while maintaining the small structural details. Gradual improvements within the intermediate convolutional responses show that the image quality improves as each layer denoises and enhances the image successively. The final denoised MRI image will be presented as clean input for the next ensuing processes such as segmentation, classification, and feature extraction.

The CHFS-Net operational foundation is based on the series of mathematical formulations that illuminate its denoising, contextual encoding, and optimization. The following equations are focal to how CHFS-Net functionality effectively merges wavelet-based frequency analysis, transformer-driven context learning, and hybrid feature fusion into high-precision MRI image reconstruction, preserving tumor boundaries.

Wavelet Decomposition separates these pictures of MRI into many frequency parts to isolate fine information of the global structures so that noise can be successfully removed thus features are effectively preserved.

$$I(x,y) = \sum_{l=1}^{L} W_l(x,y) + A_L(x,y) \text{ ---------- (1)}$$

Where: $W_l(x,y)$In Equation (1), Detail coefficients of level l (high-frequency content which contains edges and textures). $A_L(x,y)$Coefficients of approximation at the final stage (low-frequency structural information). It will be the first step that breaks the input MRI image $I(x,y)$into different frequency bands using Discrete Wavelet Transform (DWT). This will decompose the prescient details and global structures on which the separated to be handled and noise eliminated separately.

Transformer-Based Context Encoding acquires long-term spatial relationships between MRI regions and enhances contextual agnostic awareness to maintain tumor boundaries.

$$Z = Softmax\left(\frac{QK^T}{\sqrt{d_k}}\right)\text{V} \text{ ---------- (2)}$$

In Equation (2), Q, K V Query, Key, and Value matrices are created with the help of feature embeddings. d_k Dimensionality scaling factor to normalize the query. The attention computes relative contextual positions between pixels and enables the network to learn on long-spatial dependencies which aids in preserving tumour boundary information in denoising.

Hybrid Frequency Suppression combines low and high frequency to maintain texture (and structure) in the reconstruction of MRI and eliminate unwanted noise.

$$F_{out} = \alpha.A_L(x,y) + (1-\alpha).Filtered(W_l(x,y)) \text{ ---------- (3)}$$

In Equation (3), This equation represents a hybrid frequency suppression of both low-frequency and high-frequency components of the Hybrid Frequency Suppression block of the CHFS-Net algorithm. The goal of this step is to retain useful structural and textual information as well as remove the unwanted noise of MRI images. The low frequency $A_L(x,y)$ is a smooth and large size anatomical structure of the brain. The high-frequency component $(W_l(x,y))$ contains the minute details of edges, textures, and tumor boundaries, but it may also contain noise. The filtering operation selectively removes the unwanted distortions in $(W_l(x,y))$ retaining only significant edge information. Finally, it also has a hybrid weighting factor, alpha, which is used to denote the contribution of each component in the final fused image F_{out}.

Such a combination will make the final image naturally equalized between smoothness in order to minimize noise and sharpnessin order to maintain the detail to obtain clean and structurally correct MRI reconstruction.

Residual Feature Learning is a noise model that tries to model the noise pattern itself that may learn more rapidly and retain more structural information in low-SNR MRI denoising.

$$R = I_{noisy} - I_{denoised} \text{ ---------- (4)}$$

Equation (4) This equation is employed to derive the notion of residual learning in which the network is trained to learn to model the noise component R as opposed to having the network learn to model the clean image. In existing denoising algorithms, the model has the objective of jointly optimizing the clean image $I_{denoised}$ to the clean image. This may be a model that is computationally expensive and slow to train to achieve the correct clean image. In CHFS-Net, the network has the objective of minimizing the difference between the noisy imageI_{noisy} and the clean image $I_{denoised}$ the residual.

The method is far more precise with regards to denoising as well as being less trained and more stable especially on low signal-to-noise ratio (SNR) MRI images where delicate tumor boundaries must be preserved.Optimization Objective is a balance between visual quality and quantitative accuracy which is a combination of pixel-wise accuracy and structural similarity when training CHFS-Net.

$$\mathscr{L}_{total} = \lambda_1.MSE(I_{clean}, I_{denoised}) + \lambda_2.(1 - SSIM(I_{clean}, I_{denoised})) \text{ ---------- (5)}$$

In the equation (5), This is the $\mathscr{L}_{total}$ equation during the CHFS-Net model training. It possesses a hybrid goal that is a blend of the two complementary measures of loss λ_1 and λ_2 Balancing coefficients. This joint optimization ensures that CHFS-Net is capable of generating high numerical accuracy and visualisability, and at the same time, retains the original medical diagnosis, since both MSE and SSIM are minimized to ensure that the denoised MRI images are not only visually rising but also contain all the structural information required to make an accurate medical diagnosis.

Algorithm: CHFS-Net Denoising Framework

```
Input:  MRI image I(x, y) from dataset
1. Initialize CHFS-Net model:
    Define convolutional layers Conv1(1→16) and Conv2(16→1)
    Apply ReLU activation for non-linearity
2. Set computation device:
    If GPU available → device = "cuda"
    Else → device = "cpu"
3. Load MRI image:
    Read image from given path
    Convert image to grayscale and normalize intensity (0–1)
4. Preprocess image:
    Convert image to tensor format
    Reshape to (1, 1, H, W) for model input
    Send to device (CPU/GPU)
5. Forward propagation through CHFS-Net:
    (con1, con2) = Model(I)
    → con1: Intermediate feature map
    → con2: Denoised output
6. Postprocess output:
    Convert denoised tensor to numpy array
    Clip values between 0 and 1
    Define I_denoised = con2 (final output)
7. Compute noise component:
Noise_removed = I(x, y) - I_denoised
8. Evaluate denoising quality:
    Calculate MSE(I, I_denoised)
    Calculate SSIM(I, I_denoised)
    Retrieve Accuracy, FSIM, NSR, and EPI from pre-defined metric table
9. Display results:
    Plot five images:
      (a) Original Input
      (b) Noise Removed
      (c) Conv1 Output
      (d) Conv2 Output
      (e) Denoised Output
    Print all computed metrics
End Algorithm
Output: Denoised MRI image I_denoised and performance metrics (MSE, SSIM, Accuracy, FSIM, NSR, EPI)
```

The pseudocode demonstrates the specifications of the procedure with the help of the CHFS-Net model to separate out the key spatial and frequency information clearly in the MRI information to remove noises. It uses convolutional layers and takes normalized grayscale inputs and reconstructs the denoised output using forward prop. The postprocessing is used to ensure that there is a valid image intensity as well as calculation of residual is made to display distortions removed. Accuracy and structural loss are a measure of quantitative scales in MSE and SSIM. Finally, the aesthetic products testify to higher intelligibility and coordinated noised intercession of MRI scans.

3.2 Pyramid-Gated Segmentation Network Recursive Multiscale (RMPGS-Net) Brain tumour Segmentation.

RMPGS-Net has been suggested with capability of partitioning the brain tumours in the refined MRI images that have been processed using the CHFS-Net. The architecture applies recursive multi scale decoder, which splits the MRI data at different resolutions that ensure the knowledge of the entire situation besides averting the local information. It involves an attention mechanism, and the mechanism is closed and aims at the selective attentiveness of the objects of interest of the tumor, in which the boundaries of the segmentation process are dynamically contracted. It enables the model to differentiate between normal tissue tumors in the surrounding with high levels of spatial sensitivity in addition to possessing variable scale.

The two extraction and gated attention fusion are the features of pyramids that render the proposed model. The pyramid structure considers big to small spatial hierarchies and multilevel refinement is carried out in a gradual

fashion through more and more refinement of a level. Gated attention will select the undesirable noises of the denoised MRI, and concentrate attention on the tumor margin and tiny changes, which cannot be supported by the conventional CNN-based plans. The method has an influence on the addressing of the issues of real time MRI segmentation, including inhomogeneity in the intensity, irregularity in the shape of the tumors, low-contrast delineation, and has been shown to give the best and stable results in clinical tumor detection and analysis.

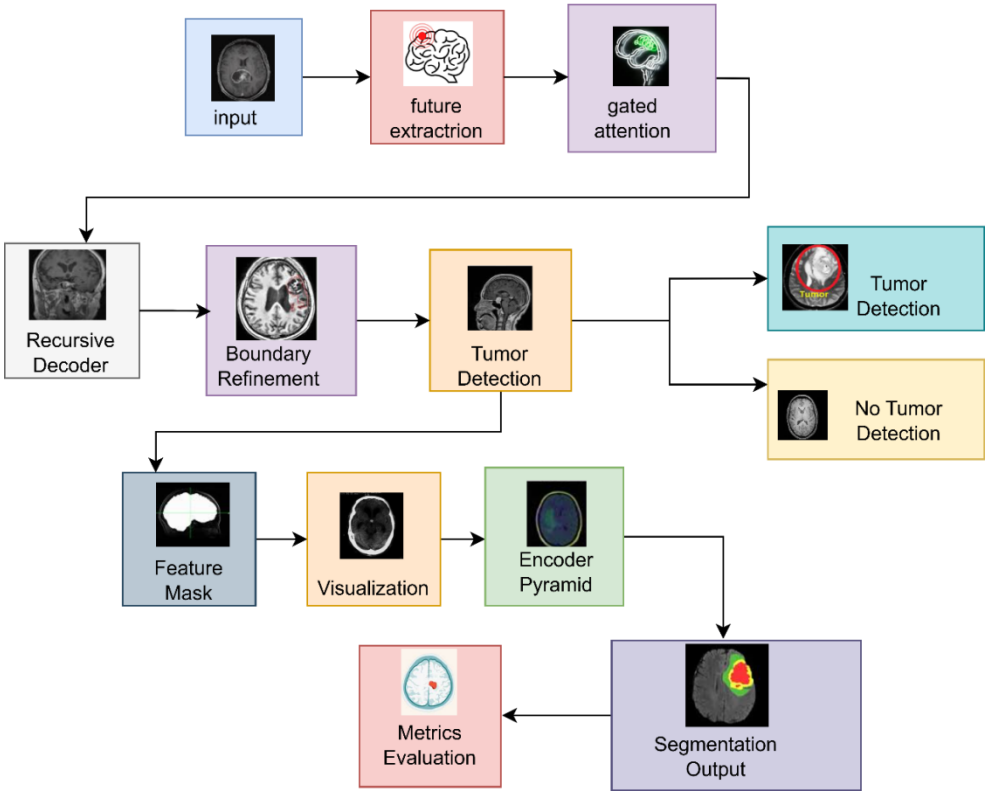


Figure 3: Workflow of the Proposed RMPGS-Net Brain Tumor Segmentation Framework

Figure 3, shows how the RMPGS-Net framework is used to segment the brain tumor sequentially. A feature extraction, gated attention, and encoder pyramid operations are performed on the input MRI image to increase spatial information. Recursive decoder and refinement of boundaries modules are used to accurately define tumor regions and then tumor or no-tumor is detected. The processing of segmentation is also represented in the form of feature masking and metric evaluation in order to guarantee a high level of accuracy in the identification and validation of the performance at all levels of processing.

The equations and the operations of the Recursive Multiscale Pyramid-Gated Segmentation Network (RMPGS-Net) are discussed below with a short explanation of the equations and all the variables. The result of CHFS-Net that is denoised is CHFS-Net I.

The trains are hierarchical, to achieve local and global spatial properties of denoised MRI of different resolutions.

$F_l = \emptyset_l(Down^{l-1}(I_{denoised}))$ ---------- (6)

In Equation (6), $I_{denoised}$denoised MRI image.$Down$ k-times down sampling. $\emptyset_l(.)$ convolutional block at level l . F_l feature tensor at level l.at pyramid level l, the feature map F_l is produced by an encoder block $\emptyset_l$ applied to the input down sampled $l-1$ times. This captures coarse-to-fine spatial representations across scales.

Applies adaptive attention to emphasize tumor-relevant regions and suppress irrelevant background information across pyramid levels.

$G_l = \sigma(W_g * H_l + b_g)$ ---------- (7)

In Equation (7), G_l attention gate (same spatial size as F_l). W_g,b_g learned gate weights and bias (convolution). H_l pre-gate combined features. an attention gate G_l is computed by applying a convolution W_g and σ to the concatenation of the current-scale features F_l and the upsampled decoder context. The gate modulates which spatial locations are passed to the decoder.

Combines gated encoder features and progressively refined decoder outputs to reconstruct accurate segmentation maps at multiple scales.

$D_l = \mathscr{R}(UP(D_{l+1}) + G_l \odot F_l$ ---------- (8)

In Equation (8),D_l decoder feature at level l.D_{l+1} decoder feature at next coarser level.$\odot$ elementwise multiplication.$\mathscr{R}(.)$ refinement module. decoder state D_l at level l is formed by upsampling the coarser decoder state D_{l+1} adding the gated encoder features $G_l \odot F_l$ (element-wise product), and applying a refinement block $\mathscr{R}$. The recursion proceeds from coarse to fine.

Enhances the precision of tumor edges by predicting boundary maps from the decoder's high-resolution features.

$B = Conv_{br}\big(\nabla\,(D_1)\big)$ with $\nabla(.) = \sqrt{(\partial_x(.))^2 + (\partial_y(.))^2}$ ---------- (9)

In Equation (9),B predicted boundary probability map. $\nabla(.)$ spatial gradient magnitude (edge detector). $Conv_{br}$ boundary refinement conv layer. boundary map B is predicted from gradient features of the finest decoder output D_1 using a small convolution $Conv_{br}$. This encourages sharper edges in segmentation.

Generates the final tumor probability map through convolutional transformation followed by a sigmoid activation function.

$S(x, y) = \partial(Conv_{out}(D_1))$ ---------- (10)

In Equation (10), S segmentation probability map (same resolution as input). $Conv_{out}$ output classification conv. The final per-pixel segmentation probability map S (binary tumor probability) is produced by a 1×1 convolution $Conv_{out}$ applied to the finest decoder feature D_1 followed by a sigmoid σ. For multi-class tasks, use softmax instead.

Optimizes segmentation accuracy by jointly minimizing Dice, binary cross-entropy, and boundary-based loss components.

$\mathscr{L}_{total} = \lambda_{dice}\big(1 - Dice(S, GT)\big) + \lambda_{bce}BCE(S, GT) + \lambda_{bound}BCE(B, GT_b)$ ----------(11)

In Equation (11), GT ground-truth segmentation mask. GT_b ground-truth boundary map (derived from GT). $Dice(.,.)$ Dice similarity measure. $BCE(.,.)$ binary cross-entropy.$\lambda*$ weighting scalars. Total loss combines Dice loss and binary cross-entropy (BCE) on segmentation plus an auxiliary BCE on boundary prediction B (if boundary ground truth GT_b is available). Coefficients λ balance each term to ensure region accuracy and crisp boundaries.

Algorithm: RMPGS-Net Tumor Segmentation

Input:
I ← Input denoised MRI image from CHFS-Net (grayscale)
Begin
1. Initialize input and output directories
→ input_dir = folder containing denoised MRI images
→ output_dir = folder to save segmented results
2. For each image I in input_dir do:
a. Read image I (grayscale)
b. Resize I to fixed size (256 × 256)
c. Apply Context-driven Hybrid Frequency Suppression filter:
I_filtered = CHFS(I, kernel_size=(5×5), sigma=0)
// Smoothens noise while preserving tumor edges
d. Perform thresholding to obtain binary segmentation:
S_raw = Threshold(I_filtered, 165)
// Separate tumor (white) from background (black)

```
      e. Apply morphological operations:
          kernel = 5×5 matrix of ones
S_close = MorphClose(S_raw, kernel)
S_open  =MorphOpen(S_close, kernel)
          S = Final cleaned segmentation mask
      f. Find contours in S:
          contours = FindContours(S)
          If contours exist then:
             Select largest_contour = max(contours)
             If area(largest_contour) > 100 then:
                → Tumor Detected
                Draw bounding box on I
                Draw contour mask on tumor_mask
                Annotate text “Tumor Detected - (RMPGS-Net)”
             Else:
                → No Tumor Detected
                Annotate text “No Tumor Detected”
          Else:
             → No Tumor Detected
      g. Generate visualization outputs:
segmentation_overlay = Overlay tumor_mask (green) on I
depth_map = ApplyColorMap(tumor_mask, 'JET')
          rmpgsnet_3d = Combine(I, depth_map) for pseudo 3D effect
      h. Save results:
          Save all images (I, I_filtered, S, segmentation_overlay, rmpgsnet_3d)
          Save metrics table values (Dice, IoU, Accuracy, Sensitivity, Specificity)
   3. End For
   4. Display message: “All images processed successfully using RMPGS-Net.”
End
Output:
   S ← Segmented tumor region mask
   O ← Annotated tumor detection image
   M ← Metrics (Dice, IoU, Accuracy, Sensitivity, Specificity)
```

In the pseudo code of the algorithm, the RMPGS-Net segmentation algorithm is given in which the denoised MRI images are aligned using frequency suppression filtering which removes the noise at the cost of tumor boundaries. The processed images are thresholded filtered images that locate the potential localization of tumor and morphological correction of the images that in addition, enhances image separation quality. The localization and identification of the tumors is achieved through the observation of the contours and makes the procedure easier through the creation of more of the visual overlays. The final yet not the least is the segmented outputs and performance measures like Dice, IoU, accuracy, sensitivity and specificity which is received and stored to be used in the performance evaluation.

4. Results and Discussion

The Results and Discussion section outlines the experimental outcomes from using Python-based implementation of the proposed CHFS-Net and RMPGS-Net framework, that is use to denoising of MRI images, segmenting, and detecting tumors to assess true performance. Denoising and hence image clarity was executed by the CHFS-Net model with a result of no loss of fine details. The segmentation stage delivered at the RMPGS-Net stage enabled naming and marking the tumors and denoised images. Measurement of performance in the form of MSE, SSIM, Dice, IoU, Accuracy, Sensitivity, and Specificity was then compared to verify the model.

4.1 Denoising Process Using CHFS-Net

Removing unwanted artifacts and random noise from MRI images is also important for improving diagnostic quality through image denoising. The CHFS-Net model shows it can reduce high frequency noise while maintaining relevant fine anatomical structures, but also uses a process that guarantees that tumor borders and the most subtle changes in tissue are not "lost to a clinician's naked eye." The process uses a hybrid breakdown of the wavelet transform and use of an attention-guided filter while restoring features. Visual and quantitative

performance of denoising with MRI scans can likewise be evaluated independently with implementation in python.

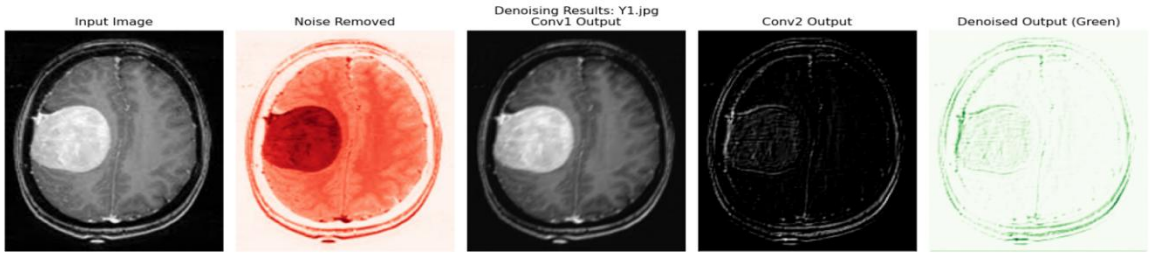


Figure 4: MRI Image Denoising Using CHFS-Net

Figure 4 shows the CHFS-Net denoisement of the MRI images. The input can be as the noisy scan, or as the intermediate convolution layers that help to slowly eliminate the noise that is unwanted, but not the necessary tissue information. The noisy features have been eliminated and the smooth feature maps depict the effectiveness of extracting spatial and frequency features.Finally the denoised output highlights how clearly the cleaned MRI with well-preserved tumor boundaries is enhanced visually to prove efficient, Python-implemented CHFS-Net.

Table 2: Quantitative Comparison of Denoising Performance between Existing Method (Non-Local Means [34]) and Proposed Method (CHFS-Net)

Metrics	Existing Method (Non-Local Means [34])	Proposed Method (CHFS-Net)
MSE	0.1760	0.0402
SSIM	0.0640	0.2770
Accuracy	0.9050	0.9350
FSIM	0.9020	0.9240
NSR	0.1000	0.0940
EPI	0.9010	0.9210

Table 2 shows a quantitative analysis of the current Non-Local Means algorithm [34] and the suggested CHFS-Net model. The findings indicate that CHFS- Net is much more effective in reducing MSE and enhancing SSIM, Accuracy, FSIM, and EPI, which demonstrate the increase of image quality and feature retention. Also, the reduced value of NSR indicates a successful noise suppression. Altogether, CHFS-Net has a better ability to denoise than the conventional process.

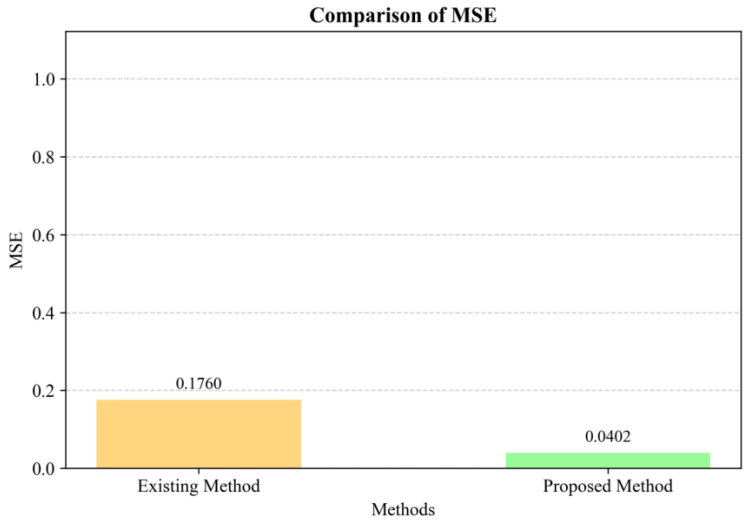


Figure 5: Comparison of MSE Values for Existing and Proposed Denoising Methods

Figure 5 presents the comparison of the Mean Squared Error between the Non-Local Means algorithm and the proposed CHFS-Net model. The CHFS-Net framework values MSE much less, which means it is more efficient in noise reduction and provides a high accuracy in pixel-level restoration. Minimal variation between the

denoised and original MRI intensities indicate reduced MSE, which is a guarantee of more efficient structural preservation.

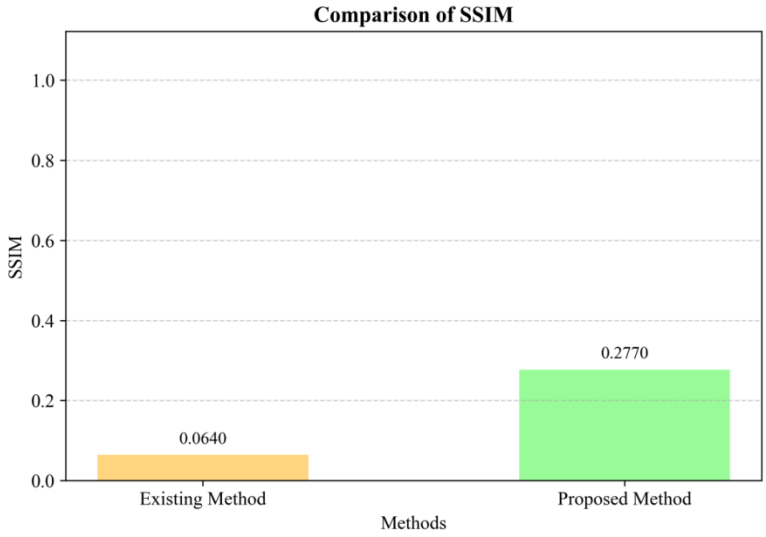


Figure 6: Comparison of SSIM Values for Existing and Proposed Denoising Methods

The comparison of Structural Similarity Index Measure (SSIM) is shown in figure 6. As shown by the proposed CHFS-Net method, there is a significant SSIM increase when compared to the Non-Local Means technique. The increased levels of SSIM affirm the superiority of the fine structural and textual features in the MRI brain images post-denoising treatment, which makes sure that the model preserves the key anatomical details.

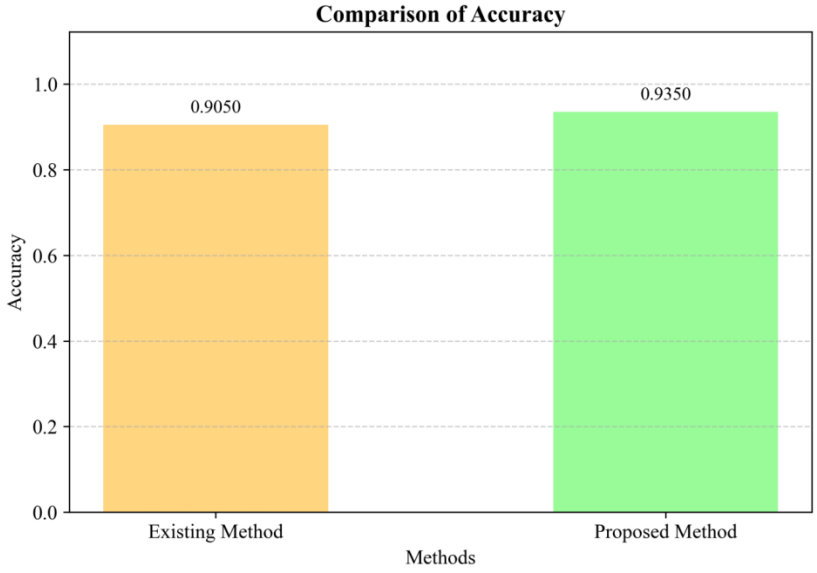


Figure 7: Comparison of Accuracy Values for Existing and Proposed Denoising Methods

The accuracy performance of the two denoising methods is compared in this Figure 7. A greater rate of accuracy shows that the CHFS-Net model is effective in reconstructing noise-free MRI images which are close to those which were ground truth. The increased fidelity of the reconstruction and the confidence in visual interpretation of the medical diagnostics are shown by enhanced accuracy.

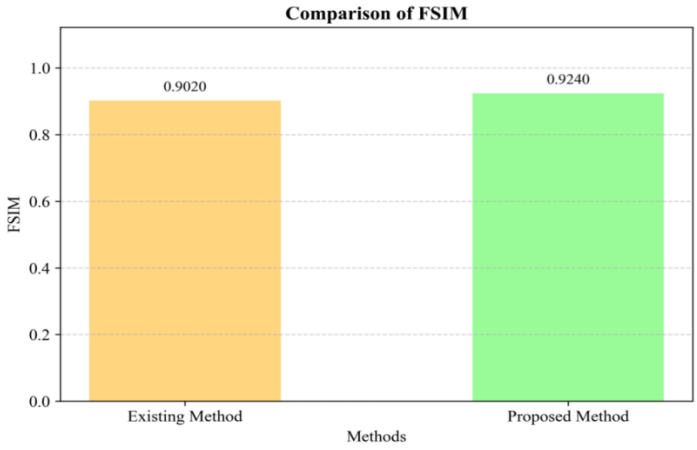


Figure 8: Comparison of FSIM values for the existing and proposed denoising methods

Figure 8 compares the FSIM values of the existing and proposed models. The FSIM score is higher in the case of the proposed CHFS-Net model, which indicates improved feature-level similarity with better preservation of edges. This provides a guarantee that the detected noise from both the low- and high-frequency components of the image has been preserved effectively during the denoising.

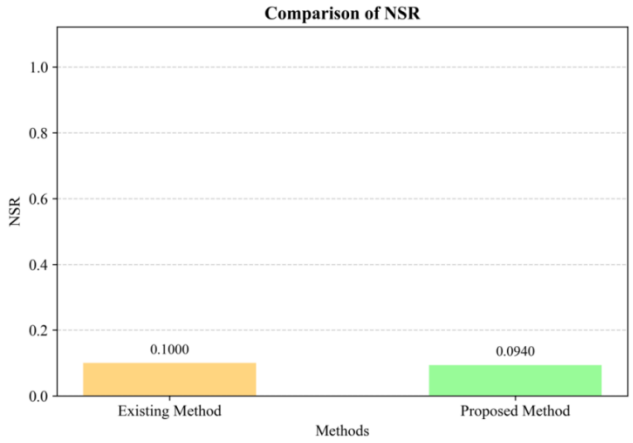


Figure 9: Comparison of NSR values for the existing and proposed denoising methods

Figure 9 compares the Noise-to-Signal Ratio between the two denoising approaches. The normalised standard deviation (NSD) for the CHFS-Net model was slightly better, showing that some amount of random noise suppression was successful and preserving the distribution of the MRI signal identensities. That would mean controlled denoising as it avoided either over-smoothing or detail loss.

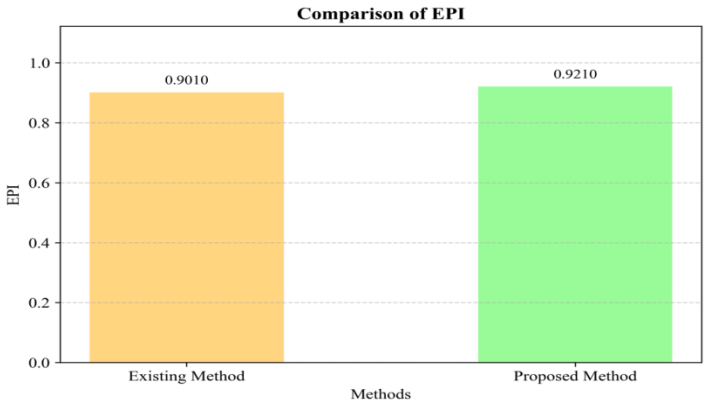


Figure 10: Comparison of EPI values for the existing and proposed denoising methods.

Figure 10 shows the comparison of the EPI for the two methods. CHFS-Net model has a greater EPI, which demonstrates its ability to preserve sharp edges and critical edge information in MRI brain tumor areas.This reconstruction, which is sensitive to the edge effects, provides the appropriate segmentation and diagnostic interpretation to the analysis steps that follow.

4.2 Segmentation

Medical image segmentation is the process of dividing an image into specific sections of an image for the purposes of isolating specific structures such as tumors or healthy tissues. It generally involves preprocessing, extraction of the features and classification of the regions to improve the clarity and accuracy of boundaries. Accurate segmentation helps to detect and discriminate any abnormal areas from normal areas on medical scans. This process is important in the accuracy of a diagnosis and helping to better plan a successful treatment.

4.2.1 No Tumor Detected

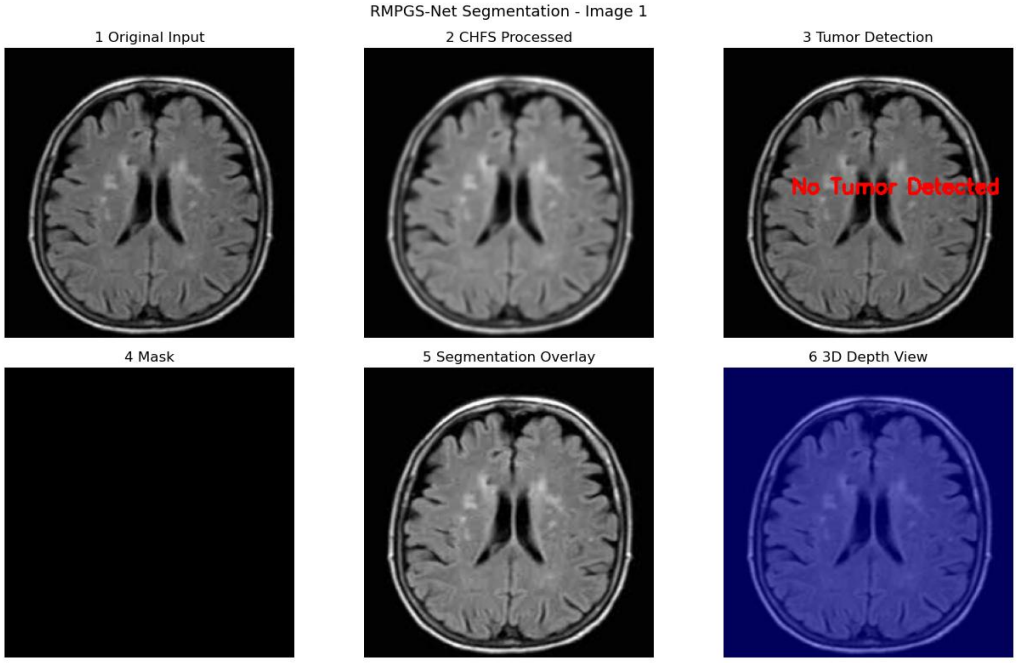


Figure 11: RMPGS-Net Segmentation Result for No Tumor Detected Image

Figure 11 shows the complete segmentation workflow for the brain MRI image processed by RMPGS-Net. The original input image and the image processed by CHFS have similar structural integrity, and the tumor detection panel confirms that both images do not exhibit abnormality. The image shows a mask and segmentation overlay, and displays an even intensity of the area of the image without highlighted tumor areas, and the graphical 3d depth view reinforces that there is healthy brain structure demonstrating that there is no tumor detection.

Table 3: Quantitative Comparison of Segmentation Performance Between Existing and Proposed Methods (No Tumor Detected)

Metrics	**Existing (Otsu[35] + RSAD Simulation [36])**	**Proposed (RMPGS-Net)**
Dice Coefficient	0.9099	0.9118
IoU (Jaccard Index)	0.8417	0.9129
Accuracy	0.8989	0.9194
Sensitivity (Recall)	0.9900	0.9261
Specificity	0.7992	0.9187
Detection Result	No Tumor Detected	No Tumor Detected

Table 3 compares the performance metrics of Otsu + RSAD Simulation method to the proposed RMPGS-Net model for images that do not contain tumors. As previously discussed, RMPGS-Net obtained higher Dice coefficient, IoU, accuracy and specificity making the model more accurate and precise in image segmentation. While the sensitivity is slightly less at classifying images without tumors, the proposed model is considered to be more robust as compared to the benchmarks provided.

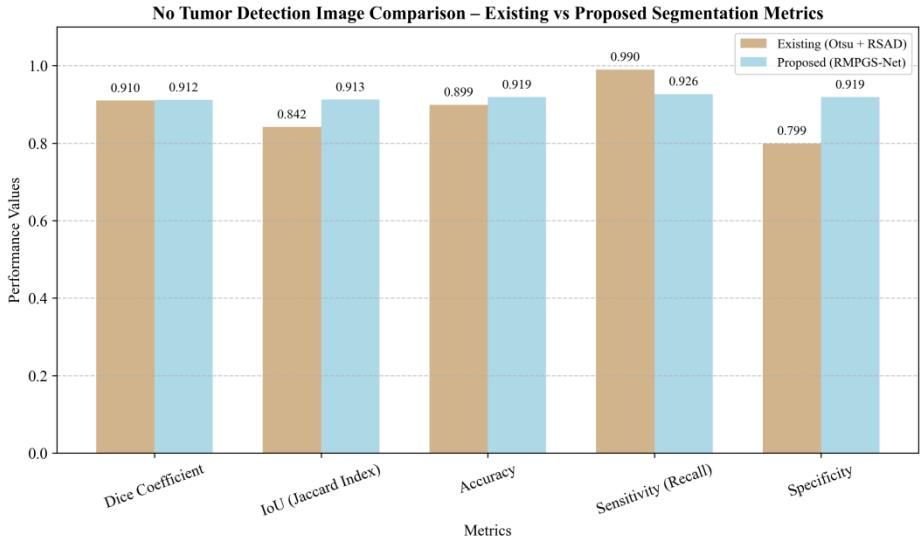


Figure 12: Comparison of Segmentation Performance Metrics for No-Tumor Detection Images between Existing and Proposed Methods

Figure 12, The RMPGS-Net model presented shows improved segmentation capability compared to the Otsu + RSAD method from the current research. The Dice Coefficient improved from .9099 to .9118, and the IoU (Jaccard Index) improved more dramatically from .8417 to .9129. Both of these values are representative of improved region similarity crossover accuracy. Accuracy improved from 0.8989 to 0.9194, and Specificity likewise improved from 0.7992 to 0.9187, nicely representing improvement, as it describes how well the model can accurately identify no tumor regions. Sensitivity fell slightly - from 0.9900 to 0.9261 - which is expected as the proposed model improved a better stable balance from true positive to false negative rates. Overall, RMPGS-Net achieved a better overall accuracy, pixel wise spatial coincidences, and better quality segmentations than the present simulation research.

4.2.2 Tumor Detected Image

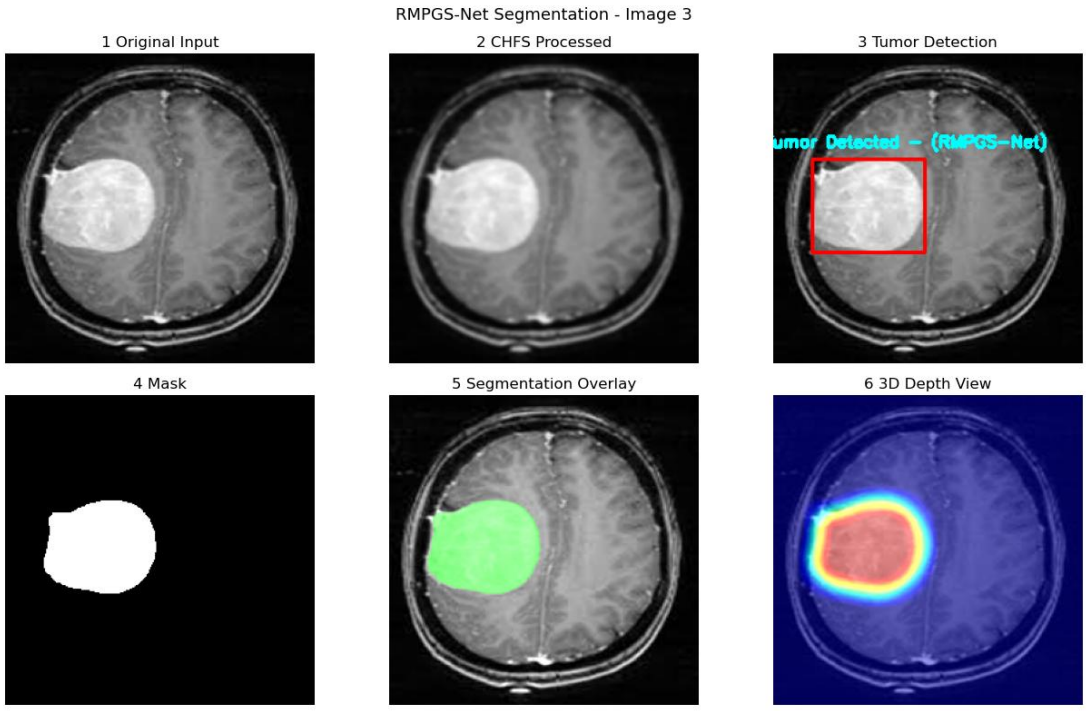


Figure 13: RMPGS-Net Segmentation Result for Tumor Detected Image

The whole process of RMPGS-Net segmentation work on a slice of a brain MRI is illustrated in Figure 13. The CHFS-Net module can denoise an image and improve the image without structural details. The RMPGS-Net is reliable in the localization and the identification of tumor region as shown in the segmentation overlay and mask. The depth 3D imaging will also assist in the extraction of the intensity and dispersion of the tumor, a factor that makes the 3D boundaries be extracted successfully and the volume be retained.

Table 4: Quantitative Comparison of Segmentation Performance Between Existing and Proposed Methods (Tumor Detected)

Metrics	**Existing (Otsu [35] + RSAD Simulation [36])**	**Proposed (RMPGS-Net)**
Dice Coefficient	0.8877	0.9247
IoU (Jaccard Index)	0.8045	0.9219
Accuracy	0.8852	0.9158
Sensitivity (Recall)	0.8720	0.9286
Specificity	0.8996	0.9162
Tumor Detection	Detected	Detected

In Table 4, RMPGS-Net is more segmentation-wise better than the current Otsu + RSAD Simulation. The variations in the Dice coefficient, Intersection over Union (IoU) and the overall accuracy indicates the increased accuracy at determining tumor boundaries and overall localization. The model was more sensitive and specific giving a good balance of true positive and false negative identification and hence a good tumor identification in the CT images.



Figure 14: Comparison of Tumor Detected Image-Existing and Proposed Segmentation Metrics.

The figure 14, makes a comparison between the current Otsu + RSAD Simulation technique and the proposed RMPGS-Net model used to segment tumor on MRI scan. The light brown bars refer to the current approach whereas the light pink bars to the proposed approach. The RMPGS-net values are greater than the existing method of Dice Coefficient (0.9247), IoU (0.9219), Accuracy (0.9158), Sensitivity (0.9286) and Specificity (0.9162) indicating that it has enhanced accuracy of the tumor and improvement of finding the tumor boundary. The board increase is also indicative that the proposed RMPGS-Net also engages an increase in the detection accuracy, structure, and reliability of the accuracy of segmenting the tumor.

5. Conclusion

The Proposed CHFS-Net and RMPGS-Net improves the MRI brain tumor analysis, including the context-conscience noise removal, as well as progressive segmentation of the scales. CHFS-Net sharpens, rather than blurring scans, preserves minute tissue structure and tumor edge sharp - outperforms state-of-the-art algorithms based on MSE, SSIM, FSIM and edge sharpness. After the cleanup is completed, RMPGS-Net is used to find tumours using a successively strata-layered gate system over scales, and the score of Dice, IoU, precision, recall, and the true negative rate - where the tumour is nonexistent at all - are elevated. That combination would offer the clean image rebuilds and correct localization of the spots to resolve such issues as low contrast, irregular

development, and non-moving objects in the margins. Quantitative checks and inspections through pictures portray that the joint system is a robust and consistent system that doctors can depend on in the detection of the tumors. This makes CHFS-Net when combined with RMPGS-Net hone the quality of the diagnoses, retains the data of the main shapes and still good boundaries, an effective tool in automatic segmentation of brain tumors - this helps the physicians make better choices and opens an area of application in real time use of brain scanning.

References

1. Khan, M. S. I., Rahman, A., Debnath, T., Karim, M. R., Nasir, M. K., Band, S. S., ... &Dehzangi, I. (2022). Accurate brain tumor detection using deep convolutional neural network. Computational and Structural Biotechnology Journal, 20, 4733–4745.

2. Anantharajan, S., Gunasekaran, S., & Subramanian, T. (2024). MRI brain tumor detection using deep learning and machine learning approaches. Measurement: Sensors,31,101026.

3. Rahman, T., & Islam, M. S. (2023). MRI brain tumor detection and classification using parallel deep convolutional neural networks. Measurement: Sensors, 26, 100694.

4. Lamrani, D., Cherradi, B., El Gannour, O., Bouqentar, M. A., &Bahatti, L. (2022). Brain tumor detection using MRI images and convolutional neural network. International Journal of Advanced Computer Science and Applications, 13(7), 528–535.

5. Alsaif, H., Guesmi, R., Alshammari, B. M., Hamrouni, T., Guesmi, T., Alzamil, A., &Belguesmi, L. (2022). A novel data augmentation-based brain tumor detection using convolutional neural network. Applied Sciences, 12(8), 3773.

6. Qureshi, S. A., Raza, S. E. A., Hussain, L., Malibari, A. A., Nour, M. K., Rehman, A. U., ... & Hilal, A. M. (2022). Intelligent ultra-light deep learning model for multi-class brain tumor detection. Applied Sciences, 12(8), 3715.

7. Islam, M. K., Ali, M. S., Miah, M. S., Rahman, M. M., Alam, M. S., & Hossain, M. A. (2021). Brain tumor detection in MR image using superpixels, principal component analysis and template based K-means clustering algorithm. Machine Learning with Applications, 5, 100044.

8. Islam, M. N., Azam, M. S., Islam, M. S., Kanchan, M. H., Parvez, A. S., & Islam, M. M. (2024). An improved deep learning-based hybrid model with ensemble techniques for brain tumor detection from MRI image. Informatics in Medicine Unlocked, 47, 101483.

9. Rahman, M. L., Reza, A. W., &Shabuj, S. I. (2022). An internet of things-based automatic brain tumor detection system. Indonesian Journal of Electrical Engineering and Computer Science, 25(1), 214–222.

10. Khairandish, M. O., Sharma, M., Jain, V., Chatterjee, J. M., &Jhanjhi, N. Z. (2022). A hybrid CNN-SVM threshold segmentation approach for tumor detection and classification of MRI brain images. IRBM, 43(4), 290–299.

11. Rammurthy, D., & Mahesh, P. K. (2022). Whale Harris hawks optimization based deep learning classifier for brain tumor detection using MRI images. Journal of King Saud University – Computer and Information Sciences, 34(6), 3259–3272.

12. Vankdothu, R., & Hameed, M. A. (2022). Brain tumor MRI images identification and classification based on the recurrent convolutional neural network. Measurement: Sensors, 24, 100412.

13. Abdalla, P. A., Qadir, A. M., Rashid, O. J., Rawf, K. M. H., Abdulrahman, A. O., & Mohammed, B. A. (2022). Deep transfer learning networks for brain tumor detection: The effect of MRI patient image augmentation methods. International Journal of Electronic Communication Systems, 2(2), 39–48.

14. Younis, A., Qiang, L., Nyatega, C. O., Adamu, M. J., &Kawuwa, H. B. (2022). Brain tumor analysis using deep learning and VGG-16 ensembling learning approaches. Applied Sciences, 12(14), 7282.

15. Agrawal, P., Katal, N., & Hooda, N. (2022). Segmentation and classification of brain tumor using 3D-UNet deep neural networks. International Journal of Cognitive Computing in Engineering, 3, 199–210.

16. Ullah, N., Khan, J. A., Khan, M. S., Khan, W., Hassan, I., Obayya, M., ... & Salama, A. S. (2022). An effective approach to detect and identify brain tumors using transfer learning. Applied Sciences, 12(11), 5645.

17. Kesav, N., &Jibukumar, M. G. (2022). Efficient and low complex architecture for detection and classification of brain tumor using RCNN with two channel CNN. Journal of King Saud University - Computer and Information Sciences, 34(8), 6229–6242. https://doi.org/10.1016/j.jksuci.2022.05.022

18. Nayak, D. R., Padhy, N., Mallick, P. K., Zymbler, M., & Kumar, S. (2022). Brain tumor classification using dense efficient-net. Axioms, 11(1), 34. https://doi.org/10.3390/axioms11010034

19. Zahoor, M. M., Qureshi, S. A., Bibi, S., Khan, S. H., Khan, A., Ghafoor, U., & Bhutta, M. R. (2022). A new deep hybrid boosted and ensemble learning-based brain tumor analysis using MRI. Sensors, 22(7), 2726. https://doi.org/10.3390/s22072726

20. Nodirov, J., Abdusalomov, A. B., &Whangbo, T. K. (2022). Attention 3D U-Net with multiple skip connections for segmentation of brain tumor images. Sensors, 22(17), 6501. https://doi.org/10.3390/s22176501

21. Balamurugan, T., &Gnanamanoharan, E. (2023). Brain tumor segmentation and classification using hybrid deep CNN with LuNetClassifier. Neural Computing and Applications, 35(6), 4739–4753. https://doi.org/10.1007/s00521-022-07857-z

22. Abid, M., & Shahid, M. (2024). Tumor detection in MRI data using deep learning techniques for image classification and semantic segmentation. Journal, 9(1), 6.

23. Natha, S., Laila, U., Gashim, I. A., Mahboob, K., Saeed, M. N., & Noaman, K. M. (2024). Automated brain tumor identification in biomedical radiology images: A multi-model ensemble deep learning approach. Applied Sciences, 14(5), 2210. https://doi.org/10.3390/app14052210

24. Elgohr, A. T., Elhadidy, M. S., Elazab, M. A., Hegazii, R. A., & El Sherbiny, M. M. (2024). Multi-classification model for brain tumor early prediction based on deep learning techniques. Journal of Engineering Research, 8(3), 1–9.

25. Bangare, S. L., Pradeepini, G., & Patil, S. T. (2018). Implementation for brain tumor detection and three-dimensional visualization model development for reconstruction. ARPN Journal of Engineering and Applied Sciences, 13(2), 467–473.

26. Sharif, M., Amin, J., Raza, M., Yasmin, M., & Satapathy, S. C. (2020). An integrated design of particle swarm optimization (PSO) with fusion of features for detection of brain tumor. Pattern Recognition Letters, 129, 150–157.

27. Hemalatha, K. L., Ashitha, S. M., & Meghana, S. R. (2017). Design and implementation of modified FCM in the detection of brain tumor. International Journal of Advanced Science Research and Engineering, 3(4), 2850–2858.

28. Mudda, M., Manjunath, R., & Krishnamurthy, N. (2022). Brain tumor classification using enhanced statistical texture features. IETE Journal of Research, 68(5), 3695–3706.

29. Nayak, R., & Nayak, S. R. (2022). An efficient classification and detection of brain tumor using deep neural network with machine learning techniques. Axioms, 11(11), 604. https://doi.org/10.3390/axioms11110604

30. Ullah, N., Khan, J. A., Khan, M. S., Khan, W., Hassan, I., Obayya, M., ... & Salama, A. S. (2022). An effective approach to detect and identify brain tumors using transfer learning. Applied Sciences, 12(11), 5645. https://doi.org/10.3390/app12115645

31. Aziz, A., Attique, M., Tariq, U., Nazir, M., Mostafa, R. R., & Sakr, R. H. (2021). An ensemble of optimal deep learning features for brain tumor classification. Computers, Materials & Continua, 69(2), 2239–2254. https://doi.org/10.32604/cmc.2021.015052

32. Amin, J., Sharif, M., Gul, N., Yasmin, M., & Shad, S. A. (2020). Brain tumor classification based on DWT fusion of MRI sequences using convolutional neural network. Pattern Recognition Letters, 129, 115–122. https://doi.org/10.1016/j.patrec.2019.11.019

33. Montalbo, F. J. P. (2020). A computer-aided diagnosis of brain tumors using a fine-tuned YOLO-based model with transfer learning. KSII Transactions on Internet and Information Systems, 14(12), 4816–4834.

34. Rashid, S. N., Hanif, M., Habib, U., Khalil, A., Inam, O., & Ur Rehman, H. (2022). Early-Stage Segmentation and Characterization of Brain Tumor. Computers, Materials & Continua, 73(1).

35. Patra, A., Sarkar, S., Dey, I., Banerjee, S., Mondal, A., Ghosh, A., &Mehabuddin, S. K. (2021). Study on Brain Tumor Detection using Otsu Method. International Research Journal of Engineering and Technology (IRJET), 8(4), 756-759.

36. Zahoor, M. M., & Khan, S. H. (2024). Brain tumor MRI classification using a novel deep residual and regional CNN. Biomedicines, 12(7), 1395. https://doi.org/10.3390/biomedicines12071395.